Preparation and antibacterial properties of aluminium oxide and silver nanocomposites

A. Ostroushko [a, *], A. Permyakova*, T. Zhulanova[a, b], A. Ermoshin[a], A. Melentsova[c], R. Mansurov[a], D. Kuznetsov[a]

[a] *Ural Federal University, Ekaterinburg, 620002 Russia*

[b] *Institute of High-Temperature Electrochemistry, Ural Branch of the Russian Academy of Sciences, Yekaterinburg, 620066 Russia*

[c] *Institute of Solid State Chemistry, Ural Branch of the Russian Academy of Sciences, Yekaterinburg, 620108 Russia*

e-mail: alexander.ostroushko@urfu.ru

Received June 27, 2024

Revised September 17, 2024

Accepted September 27, 2024

This work has demonstrated the possibility of obtaining dispersed nanocompositions based on aluminium oxide and metallic silver. The compositions can be obtained in a single reaction cycle using precursors in the form of aqueous solutions containing aluminium and silver nitrates and an organic component: polyvinyl alcohol, polyvinyl pyrrolidone, glycine, glycerol. Electron microscopy and X-ray studies have shown that silver nanoparticles are in contact with the surface of alumina aggregates containing phases of hydrated aluminium oxide, α-Al2O3, low temperature modifications of aluminium oxide. The absence of photocatalytic activity of the samples in the degradation reactions of methyl orange dye is shown. At the same time, the obtained samples of compositions possess antibacterial properties acceptable for practical application. The samples obtained from precursors with polyvinyl alcohol and polyvinylpyrrolidone, subjected to a final heat treatment at a temperature of 850 0C for 8 hours, had the best characteristics in this respect during experiments on cultures of Escherichia coli (E. coli).

Keywords: aluminium oxide, silver, nanocompositions, synthesis in combustion reactions, bactericidal properties

DOI: 10.31857/S0044457X250102e6

INTRODUCTION

Currently, much attention worldwide is focused on the research of nanosized silver particles [1-5], which possess high bactericidal properties, as well as on the development of methods for nanoparticle production [5-9]. Such nanoparticles can be used as external and local disinfectants, including as components of various compositions with organic and inorganic materials, and can also be introduced into the

internal environments of the organism. Factors such as size and morphology have a significant influence on the targeted antibacterial properties of silver nanoparticles and their interaction with living environments; this correlation is also being actively researched at present [2]. Variation in physical and chemical methods and conditions for obtaining nanoparticles leads to significant differences in the shape of such particles. The biomedical use of silver nanoparticles is not limited to the above; they can also be applied in the field of spectroscopic studies of biological objects [7, 10].

One of the relatively simple to implement and controllable methods for obtaining oxide nanostructured materials [11, 12] of various compositions and structural types, including those containing metallic silver nanoparticles [13], is synthesis in combustion reactions of nitrate-organic precursors [14-22] (Solution Combustion Synthesis – SCS). Therefore, in this work, the possibility of obtaining nano-sized silver particles by this method was studied. To prevent self-aggregation of silver nanoparticles, it was decided to use a carrier. Ceramic particles were chosen as the carrier because they are not inferior to other pharmaceutical carriers (metals, natural and synthetic polymers) in many respects and have several advantages [23]. Thus, solid particles can easily move through various body systems, such as blood vessels, digestive tract, pass through cell membranes, etc., delivering drugs no worse than their polymer analogs [24]. Ceramic particles have a large surface area to volume ratio, which ensures high drug loading, its gradual release, and prolonged action [25]. The unique properties of such carriers include resistance to biodegradation, stability in the human body with changes in pH and temperature, and biocompatibility [23]. Additionally, the production process of ceramic particles is easier, less expensive, and faster. Advances in nanotechnology allow the production of high-purity ceramic particles with a large surface area to volume ratio, as well as control over particle size, shape, and porosity [26]. Nanostructured aluminum oxide meets all the above requirements. It possesses properties such as chemical inertness in the body environment, resistance to oxidation and corrosion, mechanical strength, stability, low toxicity, and biocompatibility, making it a promising carrier for drugs, including antibacterial ones [26]. There are many methods for obtaining nanostructured aluminum oxide [27-29]. Moreover, it is possible to obtain a composite that includes silver nanoparticles and aluminum oxide in one cycle using the combustion synthesis method, which significantly simplifies the technology and saves time. Additionally, aluminum oxide-silver nanocompositions are considered as fillers for antibacterial fabric fibers and as antibacterial preparations. Consequently, obtaining such a hybrid system through a simple and accessible method will expand the possibilities for biomedical use of composites that include silver nanoparticles. The synthesis of aluminum oxide in a dispersed state in combustion reactions was studied by us earlier [30]. The obtained powders contained phases of partially hydrated aluminum oxide with the composition $Al_{10}O_{15}\cdot H_2O$ and $(Al_2O_3)_4\cdot H_2O$ (akdalite) [30] and were used as a nano-sized additive to reduce the sintering temperature of technical ceramics based on aluminum oxide. It should be noted that aluminum oxide is a biocompatible material used, for example, in dentistry and other

fields of medicine. Available data on the cytotoxicity of aluminum oxide particle aggregates, particularly in relation to tumor cells, mainly concern systems where its thin nanosheets are present [31, 32].

The purpose of this work is to study the possibility and features of synthesizing aluminum oxide-silver nanocompositions in a single reaction cycle, as well as to investigate the influence of the composition of the initial nitrate-organic precursors on the morphology and bactericidal properties of the resulting silver-containing nanocompositions.

EXPERIMENTAL PART

For the synthesis of aluminum oxide–silver nanocompositions, initial aqueous solutions containing aluminum nitrate Al(NO3)3 ·9H2O, silver nitrate AgNO3 (both "ch.d.a." qualifications), polyvinyl alcohol (PVA, medium molecular weight 11/2 GOST 10779-78, viscosity of 4% aqueous solution at room temperature) were used as precursors. 11 sDr (0.011 Pa s), the amount of residual acetate groups 2%, molecular weight 44,000), polyvinylpyrrolidone (PVP, molecular weight 40,000, Sigma-Aldrich, PVP40, CAS 9003-39-8), glycine grade "H. H." and glycerin qualification "H. D. A.". The precursor was designed to produce a composition containing 90% by weight. % aluminum oxide and 10% by weight % metallic silver. The stoichiometric ratio of the organic component and nitrates was calculated based on gorenje reactions (1)–(8) with the formation of nitrogen, carbon dioxide, and water vapor as gaseous products

$$2Al(NO_3)_3 + 3(C_2H_4O) = Al_2O_3 + 6CO_2 + 3N_2 + 6H_2O, \quad (1)$$

$$10AgNO_3 + 6(C_2H_4O) = 10Ag + 12CO_2 + 5N_2 + 12H_2O, \quad (2)$$

$$62Al(NO_3)_3 + 30(C_6H_9NO) = 31Al_2O_3 + 180CO_2 + 108N_2 + 135H_2O, \quad (3)$$

$$62AgNO_3 + 12(C_6H_9NO) = 62Ag + 72CO_2 + 37N_2 + 54H_2O, \quad (4)$$

$$6Al(NO_3)_3 + 10C_2H_5NO_2 = 3Al_2O_3 + 20CO_2 + 14N_2 + 25H_2O, \quad (5)$$

$$6AgNO_3 + 4C_2H_5NO_2 = 6Ag + 8CO_2 + 5N_2 + 10H_2O, \quad (6)$$

$$14Al(NO_3)_3 + 15C_3H_8O_3 = 7Al_2O_3 + 45CO_2 + 21N_2 + 60H_2O, \quad (7)$$

$$14AgNO_3 + 6C_3H_8O_3 = 14Ag + 18CO_2 + 7N_2 + 24H_2O. \quad (8)$$

When writing reactions and in calculations, molecular oxygen from the air was not taken into account, since these combustion reactions can proceed in its absence due to the internal oxidizer in the precursor (nitrate). In addition, even when conducting the reaction in air, the portion of the precursor that is not on the surface and tightly adheres to the reactor walls does not have access to the oxygen in the surrounding air. Therefore, to describe such redox reactions (combustion of precursors) with an internal oxidizer and "fuel," various degrees of formalized reactions can be used [33], in which the nitrate part of the acidic composition is accounted for as nitric acid. To prepare the precursors,

two working solutions were prepared separately, containing nitrates of the corresponding metals and an organic component. Metal nitrate solutions were prepared by dissolving pre-calculated weights based on the combustion reaction in distilled water. Solutions of polymeric components (PVA or PVP concentration 5 and 10 wt. % respectively) were prepared by heating in a water bath. Glycine and glycerin solutions were obtained by dissolving weights calculated from the combustion reaction in distilled water. The intermediate concentrations of the solutions were not determined. After mixing the nitrate solution and the solution of one of the organic components, the total solution was brought to the 250.0 cm^3 mark with distilled water. Combustion of precursors was carried out in porcelain dishes with heating on an electric hot plate to initiate the combustion process. Depending on the type of organic component, the combustion initiation temperature varied in the range of 200–250°C. Final heat treatment was carried out in a high-temperature furnace. At the first stage, firing was carried out for 8 hours at a temperature of 650°C. Then each of the obtained samples was divided into two parts. The first part was studied without additional heat treatment, while the second part of the samples was additionally kept at a temperature of 850°C for 8 hours to study the effect of the final heat treatment temperature on the phase composition, size, and morphology of the composite particles. X-ray phase analysis of the samples was performed on a D8 Advance diffractometer using Cu K_α-radiation in the angle range $20° \leq 2\theta \leq 80°$. Electron microscopy of the samples was carried out using a Jeol JSM 6390 transmission electron microscope with a JED 2300 attachment.

To evaluate antibacterial activity, a weighed sample, ground in a mortar and sieved, was added directly to the culture medium before autoclaving. The reference sample – silver nitrate – was added after autoclaving before pouring the media, when the temperature was 6–50°C. For the experiments, LB nutrient medium without sodium chloride (10 g/L tryptone and 5 g/L yeast extract) with 1.5% agar was used. Autoclaving was carried out for 20 minutes at 115°C. A culture of *E. coli* , strain TG-2, was used. The overnight bacterial culture was diluted 10^8 times, after which 50 μL of the diluted bacterial suspension was spread with a Drigalski spatula on the test medium – 20 mL in a 10 cm diameter Petri dish. The next day, the grown colonies were counted (in 3 × 3 cm sections). The measurements were repeated 5 times. The significance of differences from the control variant without the addition of powder sample or silver nitrate was determined using the non-parametric Mann-Whitney U-test. Photography was performed on the second day to make the colonies more visible. The optimal volume of culture introduced and the degree of its dilution were selected in a preliminary experiment. The tested concentration of silver ions and its nanoparticles was 0, 0.4, 1.0, and 2.5 mM/L, taking into account its content in the samples of 10 wt%.

RESULTS AND DISCUSSION

During the synthesis of samples from precursors with PVA, PVP, glycine, and

glycerol, alumina-silver dispersed compositions were obtained, containing particles and nanostructured aggregates based on aluminum oxide with silver nanoparticles of different morphologies on their surface (Fig. 1, 2). Ensembles of associated particles based on aluminum oxide have sizes acceptable for biomedical use (10-200 μm), with distinguishable individual particles of 1-5 μm within the ensembles. In this case, biomedical use implies the application of these composites as fillers for antibacterial fabric fibers and local antiseptic preparations. The specified particle size range (1-200 μm) is acceptable for using composites for these purposes [34]. According to X-ray phase analysis, in addition to metallic silver, the nanostructured aggregates contain such Al-containing phases as hydrated aluminum oxide [30], α-Al_2O_3, low-temperature modifications of Al_2O_3. The microphotographs show that silver nanoparticles are distributed over the aluminum oxide surface, closely adhering to this surface. The size and shape of silver particles, as well as the nature of their distribution over aluminum oxide particle aggregates, largely depend on the organic component used in the synthesis. For instance, in samples obtained from precursors with PVA and PVP at 650 and 850 °C (Fig. 1a-1d, 2a-2d), silver particles have a plate-like shape, with sizes varying in the range of 1-10 μm. In the sample obtained with glycerol at 850 °C (Fig. 2g, 2h), silver plates have smaller sizes and a needle-like shape. In samples synthesized using glycine (Fig. 1e, 1f, 2e, 2f), silver particles were strongly aggregated on the aluminum oxide surface, forming aggregates from 1-5 μm. With increasing final heat treatment temperature of samples with PVA and glycerol, the sizes of aluminum oxide particle aggregates and silver plates located on them decreased, while for samples with PVP and glycine, they increased. In the microphotographs, silver appears lighter. In addition to the plate-like silver forms described above, the samples contain nanoscale particles of a more rounded shape (Fig. 1, 2). Such particles range from 10 to 100 nm, which fits into the generally accepted concepts of nanoscale objects. It can be assumed that the presence of metallic silver formations of different morphologies and sizes in the obtained composite material contributes to enhancing the bactericidal properties of the material at different stages of its impact on biological environments. The smallest nanoparticles provide the necessary rapid action against harmful bacteria in the first moments of contact with the biological environment, while larger nanoparticles can maintain the long-term dynamics of prolonged bactericidal effects.

The presence of nanoscale silver particles and their uniform distribution on the surface of aluminum oxide particles and aggregates were determined using energy-dispersive analysis (Fig. 3, 4).

X-ray phase analysis of the samples showed the presence of metallic silver (COD ID: 1100136) in all studied samples (Fig. 5). In samples heat-treated at 650°C, the presence of mixed phases of hydrated aluminum oxide can be assumed (Fig. 5a, 5b), whereas for samples maintained at 850°C (Fig. 5c, 5d), such Al-containing phases as hydrated aluminum oxide [30], α-Al_2O_3 (COD ID: 1000017), and low-temperature modifications of Al_2O_3 were found. The low-temperature modifications of aluminum oxide include γ-, η-, and χ-Al_2O_3, obtained by calcination at a temperature of 500–

700°C of boehmite, bayerite, and hydrargillite, respectively [31, 32, 35]. The difference between low-temperature modifications of aluminum oxide is negligible, and there is no reliable identification method [36], therefore, within the framework of this work, the content of specific low-temperature modifications was not determined. In the experimental X-ray diffraction patterns (Fig. 5c, 5d), the possibility of forming the high-temperature phase α-Al_2O_3 is indicated by maxima at scattering angles of ~25° and ~35°, which are not characteristic of low-temperature modifications [37]. The presence of spinel-type modifications is indicated by maxima at ~34° and ~39°, which are not characteristic of α-Al_2O_3 [38]. The appearance of a maximum at ~20° (Fig. 5d) indicates that some aluminum atoms occupy "non-spinel" positions [38].

Evaluation of the antibacterial activity of the obtained nanocompositions showed positive results (Fig. 6). As expected, the synthesis conditions of the compositions affect their target properties. Compositions obtained from precursors containing PVA and PVP as an organic component, whose final heat treatment was carried out at a temperature of 850°C, possess maximum bactericidal characteristics; they inhibit the growth of *E. coli* colonies similar to silver nitrate (Table 1). Additionally, with an increase in the final heat treatment temperature, an increase in antibacterial activity is observed for all compositions. Samples of aluminum oxide obtained under conditions similar to these compositions, but not containing silver, do not possess bactericidal activity under the conditions of the conducted experiments. It should be noted that in the temperature range of heat treatment of the obtained samples, dehydration of aluminum oxide occurs, as evidenced by the appearance of its anhydrous forms. It cannot be excluded that during this process, the formation of aluminum oxide particles with the most optimal properties, having the form of plates, occurs as a carrier for highly dispersed silver. Silver particles in this case also acquire the form of nanoplates. The authors [39] note increased cytotoxicity of particles in the form of nanoplates. At the same time, higher heat treatment temperatures as they approach the melting point of silver will lead to its self-aggregation. Therefore, the upper range was limited to 850°C. Thus, it can be assumed that a morphology is more preferable in which silver particles in the form of thin small plates closely adhere to the aggregates of aluminum oxide particles, distributing over their surface, which is observed in the case of PVA and PVP samples held at a higher temperature. The experimental results show that the obtained compositions have prospects for use, for example, as a filler for antiseptic materials.

Table 1 presents for comparison the values of antibacterial activity of silver nitrate solution as an effective bactericidal agent used in medicine as a local antiseptic, antibacterial drug, etc. [40]. The data on colony growth for aluminum oxide containing no silver additives is presented. The obtained data indicate the absence of antibacterial activity in pure aluminum oxide.

It is important to note a key point. Obtaining aluminum oxide-silver compositions in one cycle simplifies the technology, saving time and energy. In addition, the combustion process of nitrate-organic precursors releases significantly less harmful substances (carbon monoxide, nitrogen oxides) [12] into the environment

compared to, for example, thermal decomposition of salt forms themselves. This is achieved through the redox interaction of precursor components simultaneously with the catalytic effect of intermediate and target solid-phase products on the released gaseous products [11]. In particular, this may initiate a reaction between carbon monoxide and nitrogen oxides to form molecular nitrogen and low-toxic carbon dioxide [11].

CONCLUSION

The conducted studies have established the possibility of obtaining nanocompositions containing aluminum oxide and metallic silver particles from nitrate-organic precursors in a single reaction cycle. Such compositions have particle sizes acceptable for practical application and high bactericidal activity, which has been demonstrated in experiments with Escherichia coli (*E. coli*) cultures. The biological activity of the obtained samples varies depending on the conditions of their preparation. The materials obtained from precursors with PVA and PVP after additional heat treatment at 850°C possess the best characteristics. The synthesis of antibacterial compositions in a single cycle from nitrate-organic precursors through the implementation of their combustion process followed by heat treatment simplifies the production method and reduces harmful emissions into the atmosphere, creating savings in time and energy costs. The majority of available literature data indicates the relative safety of aluminum oxide for animal and human organisms, although there is some information about its negative effects [41]. Therefore, one of the most promising areas for the application of this composite with bactericidal properties may be its use as a filler for antibacterial fibers (fabrics).

Possible mechanisms of silver's bactericidal action include the generation of reactive oxygen species in water-containing media [1]. For this reason, it is of interest to study the possibility of testing the photocatalytic activity of silver nanoparticles of various morphologies in relation to the degradation (decolorization) reactions of organic dyes [42, 43], similar to Fenton reactions [35, 44], as well as (if such activity is established) comparing it with antibacterial properties. In this regard, a promising research direction is the development of an indirect method for evaluating bactericidal activity based on the photocatalytic activity of silver-containing materials.

FUNDING

The research was supported by the state assignment of the Ministry of Science and Higher Education of the Russian Federation (project No. 123031300049-8).

CONFLICT OF INTEREST

The authors declare that they have no conflict of interest.

REFERENCES

1. *Gabrielyan L.S., Trchounian A.A.* // J. Belarus. State University. Biology . 2020. V. 3. P. 64. https://doi.org/10.33581/2521-1722-2020-3-64-71
2. *Meleshko A.A., Afinogenova A.G., Afinogenov G.E. et al.* // Russ. J. Infection Immunity. 2020. V. 10. № 4. P. 639. https://doi.org/10.15789/2220-7619-AIA-1512 .
3. *Dorovskikh S.I., Vikulova E.S., Sergeevichev D.S. et al.* // Coatings. 2023. V. 13. P. 1269. https://doi.org/10.3390/coatings13071269.
4. *Smolle M.A., Bergovec M., Scheipl S. et al.* // Scient. Rep. 2022. V. 12. P. 13041. https://doi.org/10.1038/s41598-022-16707-0 .
5. *Sergeevichev D.S., Dorovskikh S.I., Vikulova E.S. et al.* // Int. J. Mol. Sci. 2024. V. 25. № 2. P. 1100. https://doi.org/10.3390/ijms25021100.
6. *Krutyakov Yu.A., Kudrinskiy A.A., Olenin A.Yu., Lisichkin G.V.* // Russian Chemical Reviews. 2008. V. 82. № 3. P. 242.
7. *Stepanov A.L.* // Technical Physics. 2004. V. 74. № 2. P. 1.
8. *Speshilov I.O., Vartanyan M.A., Vagramyan T.A.* // Advances in Chemistry and Chemical Technology. 2016. V. 30. № 3. P. 59.
9. *Zakatilova E.I., Uyanga T., Merkushkin A.O., Obruchikov A.V.* // Advances in Chemistry and Chemical Technology. 2014. V. 28. № 6. P. 95.
10. *Maksimov G.V., Sazontova T.G., Kovalenko S.S. et al.* // Moscow University Chemistry Bulletin. 2015. V. 56. № 3. P. 158.
11 . *Ostroushko A.A., Russkikh O.V.* // Nanosyst.: Phys. Chem. Math. 2017. V. 8. № 4. P. 476. https://doi.org/10.17586/2220-8054-2017-8-4-476-502
12. *Ostroushko A.A., Maksimchuk T.Y., Permyakova A.E., Russkikh O.V.* // Russ. J. Inorg. Chem. 2022. V. 67. № 6. P. 799. https://doi.org/10.1134/S0036023622060171
13. *Ostroushko A.A., Adamova L.V., Koveza E.V. et al.* // Russ. J. Phys. Chem. 2018. V. 92. № 1. P. 516–521. https://doi.org/10.1134/S0036024418030214
14. *Varma A., Mukasyan A.S., Rogachev A.S., Manukyan K.V.* // Chem. Rev. 2016. V. 116. № 23. P. 14493. https://doi.org/10.1021/acs.chemrev.6b00279
15. *Chick L.A., Pederson L.R., Maupin G.D. et al.* // Mater. Lett. 1990. V. 10. № 12. P. 6. https://doi.org/10.1016/0167-577X(90)90003-5
16. *Aruna S.T.* Solution combustion synthesis. Concise Encyclopedia of Self Propagating High Temperature Synthesis. 2017. P. 344.
17. *Popkov V.I., Almjasheva O.V., Nevedomskyi V.N. et al.* // Ceram. Int. 2018. V. 44. № 17. P. 20906. https://doi.org/10.1016/j.ceramint.2018.08.097
18. *Martinson K.D., Belyak V.E., Sakhno D.D. et al.* // J. Alloys Compd. 2022. V. 894. P. 162554. https://doi.org/10.1016/j.jallcom.2021.162554

19. *Ostroushko A.A., Russkikh O.V., Maksimchuk T.Yu.* // Ceram. Int. 2021. V. 47. № 15 . P. 21905. https://doi.org/10.1016/j.ceramint.2021.04.20
20. *Lomanova N.A., Tomkovich M.V., Danilovich D.P. et al.* // Inorg. Mater. 2020. V. 56. № 12. P. 1271. https://doi.org/10.1134/S0020168520120110
21. *Popkov V.I., Almjasheva O.V., Semenova A.S. et al.* // J. Mater. Sci: Materials in Electronics. 2017. V. 28. № 10. P. 7163. https://doi.org/10.1007/s10854-017-6676-1
22. *Almjasheva O.V., Lomanova N.A., Popkov V.I. et al.* // Nanosyst.: Phys. Chem. Math. 2019. V. 10. № 4. P. 428. https://doi.org/10.17586/2220-8054-2019-10-4-428-437
23. *Zang S., Chang S., Shahzad M.B. et al.* // Rev. Adv. Mater. Sci. 2019. V. 58. P. 82. https://doi.org/10.1515/rams-2019-0010
24. *Wilczewska A.Z., Niemirowicz K., Markiewicz K.H. et al.* // Pharmacol. Rep. 2012. V. 64. № 5. P. 1020. https://doi.org/10.1016/S1734-1140(12)70901-5
25. *Kapoor S., Hegde R., Bhattacharyya A.J.* // J. Control. Release. 2009. V. 140. № 1. P. 34. https://doi.org/10.1016/j.jconrel.2009.07.015
26. *Das S.K., Kapoor S., Yamada H. et al.* // Micropor. Mesopor. Mat. 2009. V. 118. № 1–3. P. 267. https://doi.org/10.1016/j.micromeso.2008.08.042
27. *Dobrovolsky D.S., Belovoshchev N.A., Nasyrova L.A. et al.* // Advances in Chemistry and Chemical Technology. 2017. V. 31. № 13. P. 31.
28. *Fedoročková A., Sučik G., Plešingerová B. et al.* // RSC Adv. 2020. V. 10. P. 32423. https://doi.org/10.1039/D0RA06544G
29. *Lyamina G.V., Ilela A.E., Dvilis E.S. et al.* // Butlerov Readings. 2013. V. 33. No. 3. P. 55.
30. *Ostroushko A.A., Vylkov A.I., Zhulanova T.Yu. et al.* // Physical and Chemical Aspects of Studying Clusters, Nanostructures and Nanomaterials. 2023. V. 15. P. 799. https://doi.org/10.26456/pcascnn/2023.15.799
31. *Petina L.P., Levinter M.E.* // Izv. VUZov. Chemistry and Chemical Technology. 1980. V. 23. No. 4. P. 919.
32. *Gates B.K., Katzer J.R., Schuit G.C.A.* Chemistry of Catalytic Processes. N.Y.: McCraw-Hill Book Company, 1979. 464 p.
Gates B., Katzer J., Schuit D. Chemistry of Catalytic Processes. Moscow: Mir, 1981. 342 p.
33. *Ostroushko A.A.* // Inorg. Mater. 2004. V. 40. No. 3. P. 259. https://doi.org/10.1023/B:INMA.0000020524.35838.de
34. *Galimzyanova R.Yu.* Modern Composite Materials in Medical Equipment Production. Kazan, 2021. 89 p.
35. *Lippens B.C., Steggerda J.J.* Active Alumina. Structure and Properties of Adsorbents and Catalysts / Ed. by Linsen B.N. Moscow: Mir, 1973. 288 p.
36. *Chukin G.D.* Structure of Aluminum Oxide and Hydrodesulfurization Catalysts . Reaction Mechanisms . Moscow, 2010. 288 p.
37. *Baksheev E.O.* Development of Production Technology for Three-Way Catalysts

with High Catalytic Activity and Resistance to Thermal Deactivation. PhD Thesis in Technical Sciences. Ekaterinburg, 2023. https://elar.urfu.ru/bitstream/10995/128095/1/urfu2579_d.pdf ; urfu2579_d.pdf .
38. *Aleshina L.A., Sidorova O.V., Strunevskaya A.L.* // Proceedings of the Kola Science Center RAS. 2018. V. 9. No. 2. P. 498. https://doi.org/10.25702/KSC.2307-5252.2018.9.1.498-502
39. *Korovin M.S., Fomenko A.N., Bakina O.V., Lerner M.I.* // Siberian Journal of Oncology. 2016. V. 15. No. 6. P. 35. https://doi.org/10.21294/1814-4861-2016-15-6-35-41
40. *Privolnev V.V., Zabrosaev V.S., Danilenkov N.V.* // Bulletin of Smolensk State Medical Academy. 2015. V. 14. No. 3. P. 85.
41. *Zaitseva N.V., Zemlyanova M.A., Stepankov M.S., Ignatova A.M.* // Human Ecology. 2018. No. 5. P. 9.
42. *Thomas J., Periakaruppan P., Thomas V. et al.* // RSC Adv. 2018. V. 8. P. 41288. https://doi.org/10.1039/C8RA08893D
43. *Zhang Y., Liu J., Kang Y.S. et al.* // Nanoscale. 2022. V. 14. P. 11909. https://doi.org/10.1039/D2NR02665A
44. *Rozhentsev D.A., Mansurov R.R., Tkachev N.K. et al.* // Physical and chemical aspects of studying clusters, nanostructures and nanomaterials. 2021. V. 13. P. 919. https://doi.org/10.26456/pcascnn/2021.13.919

Table 1. Effect of preparations on test culture growth, percentage ratio of colony forming units in the sample to colony forming units in the control experiment

Sample	[Ag], mM			
	0	0.4	1	2.5
Control (no additives)	100 ± 2.2	–	–	–
Al_2O_3	100 ± 2.3	–	–	–
$AgNO_3$	100 ± 2.2	100 ± 8.6	52.8 ± 4.4 *	0 ± 0 *
Al_2O_3 (90 wt.%), Ag (10 wt.%), PVP, 8 h, 650 °C	100 ± 2.2	48.5 ± 7.8 *	0 ± 0 *	0 ± 0 *
Al_2O_3 (90 wt.%), Ag (10 wt.%), PVA, 8 h, 650 °C	100 ± 2.2	77 ± 12 *	0 ± 0 *	0 ± 0 *
Al_2O_3 (90 wt.%), Ag (10 wt.%), glycine, 8 h, 650 °C	100 ± 2.2	77.6 ± 7 *	85 ± 4.5 *	0 ± 0 *
Al_2O_3 (90 wt.%), Ag (10 wt.%), glycerol, 8 h, 650 °C	100 ± 2.2	81.6 ± 4 *	75 ± 2 *	0 ± 0 *
Al_2O_3 (90 wt.%), Ag (10 wt.%), PVP, 8 h, 650 °C; 8 h, 850 °C	100 ± 2.2	0 ± 0 *	0 ± 0 *	0 ± 0 *
Al_2O_3 (90 wt.%), Ag (10 wt.%) PVA, 8 h, 650 °C; 8 h, 850 °C	100 ± 2.2	0 ± 0 *	0 ± 0 *	0 ± 0 *
Al_2O_3 (90 wt.%), Ag (10 wt.%), glycine, 8 h, 650°C; 8 h, 850°C	100 ± 2.2	81.7 ± 3 *	0 ± 0 *	0 ± 0 *
Al_2O_3 (90 wt.%), Ag (10 wt.%), glycerol, 8 h, 650°C; 8 h, 850°C	100 ± 2.2	69 ± 10 *	0 ± 0 *	0 ± 0 *

* Differences are significant from control at $p < 0.01$.

FIGURE CAPTIONS

Fig. 1. SEM images of Al_2O_3-Ag samples synthesized from precursors with different organic components: a, b - PVA, 650 °C; c, d - PVP, 650 °C; e, f - glycine, 650 °C; g, h - glycerol, 650 °C.

Fig. 2. SEM images of Al_2O_3-Ag samples synthesized from precursors with different organic components: a, b - PVA, 850 °C; c, d - PVP, 850 °C; e, f - glycine, 850 °C; g, h - glycerol, 850 °C.

Fig. 3. Energy dispersive analysis results of Al_2O_3-Ag sample, PVP, 650 °C: a - SEM image; chemical element distribution maps: b - Al, c - Ag, d - O; e - energy dispersive spectrum.

Fig. 4. Energy dispersive analysis results of Al_2O_3-Ag sample, glycerol, 850 °C: a - SEM image; chemical element distribution maps: b - Al, c - Ag, d - O; e - energy dispersive spectrum.

Fig. 5. X-ray diffraction patterns of Al_2O_3-Ag samples synthesized from precursors with different organic components: a - PVA, 650 °C; b - PVP, 650 °C; c - PVA, 850 °C; d - PVP, 850 °C (line diagrams indicate phases of metallic silver (COD ID: 1100136) (black), α-Al_2O_3 (COD ID: 1000017) (blue)).

Fig. 6. Concentration dependences of the percentage ratio of colony-forming units in the studied samples synthesized with different organic components to the number of colony-forming units in the control experiment.

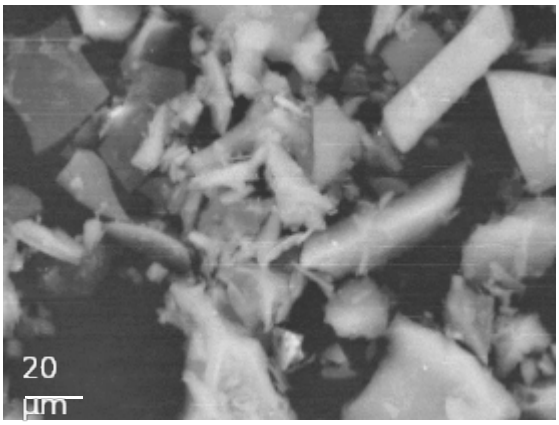

a

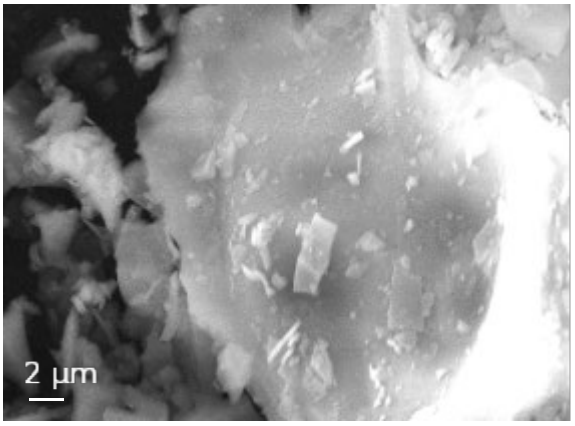

b

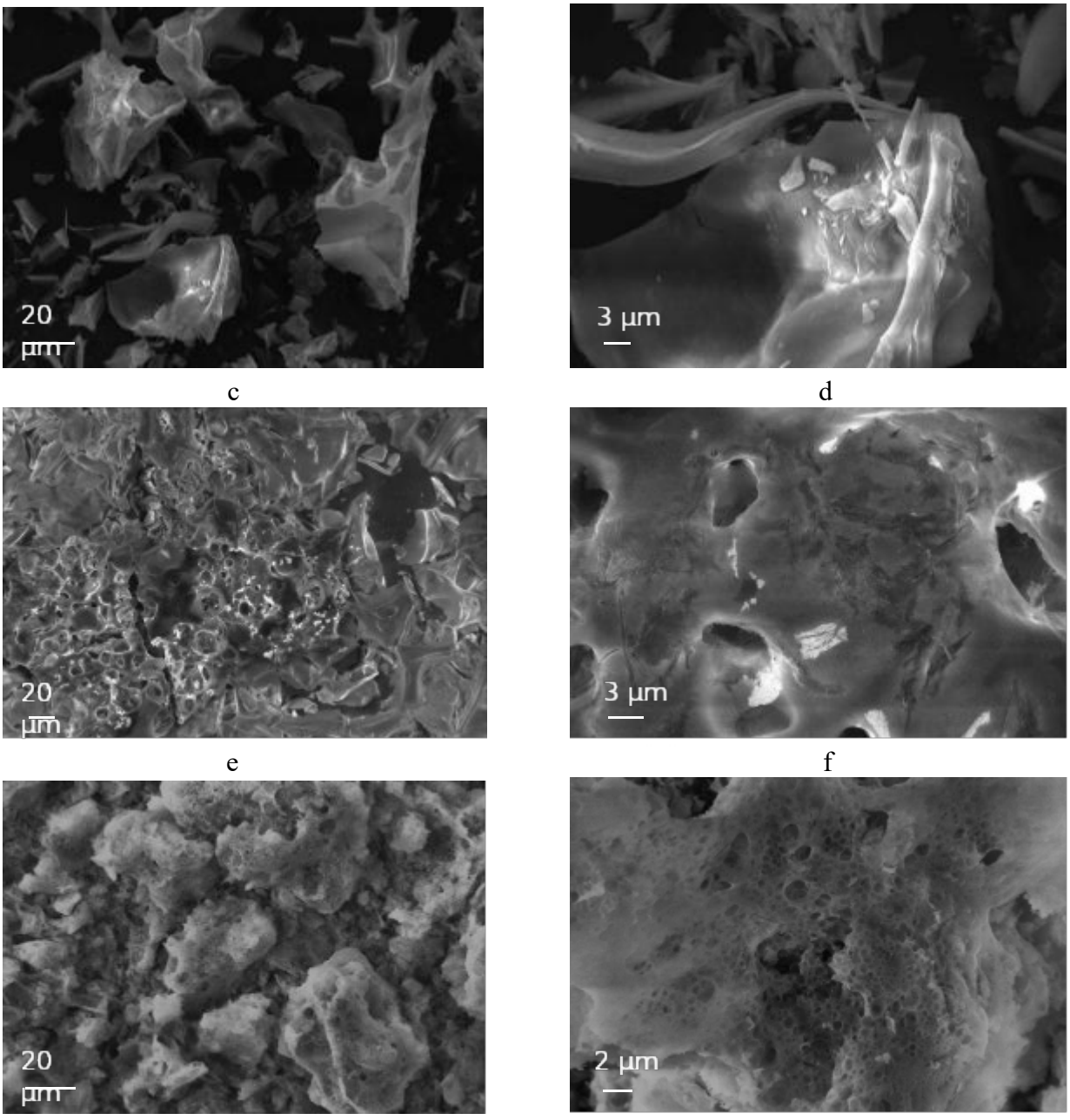

c d e f g h

Fig. 1. SEM images of Al_2O_3–Ag samples synthesized from precursors with various organic components: a, b – PVA, 650 °C; c, d – PVP, 650 °C; e, f – glycine, 650 °C; g, h – glycerol, 650 °C.

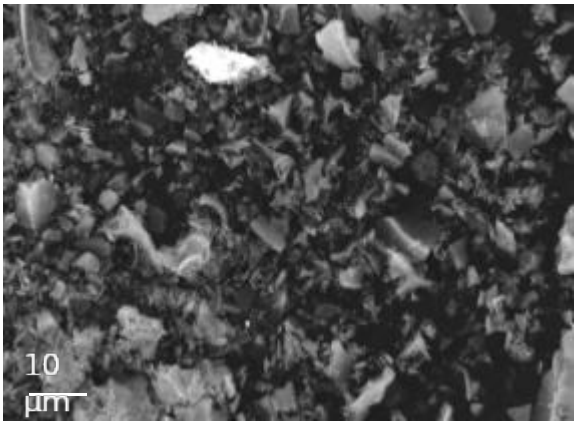

a

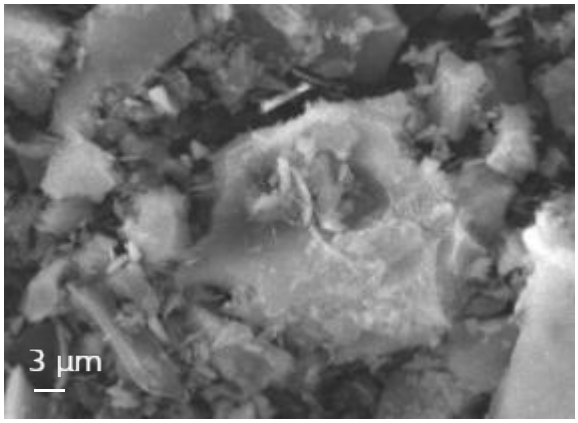

b

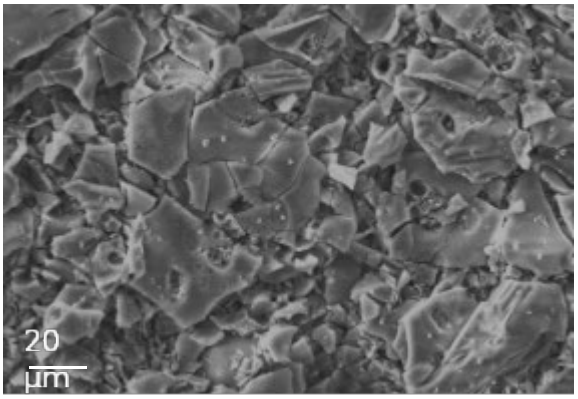

c

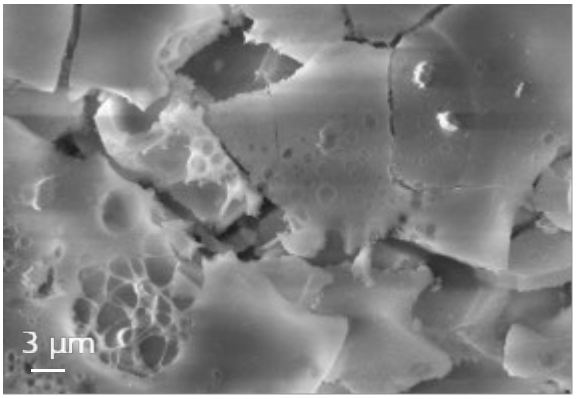

d

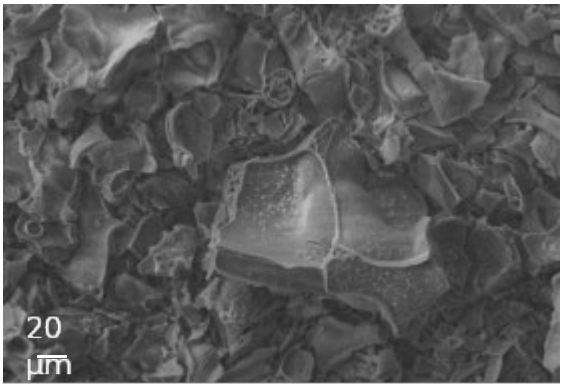

e

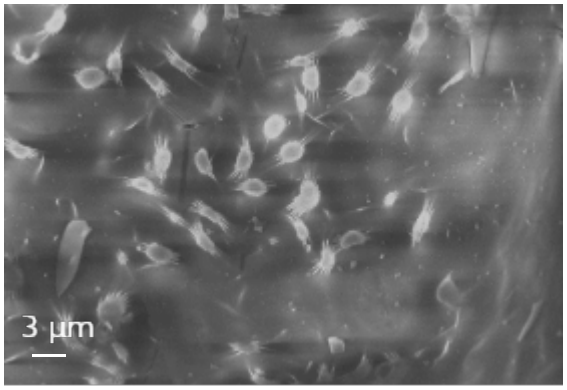

f

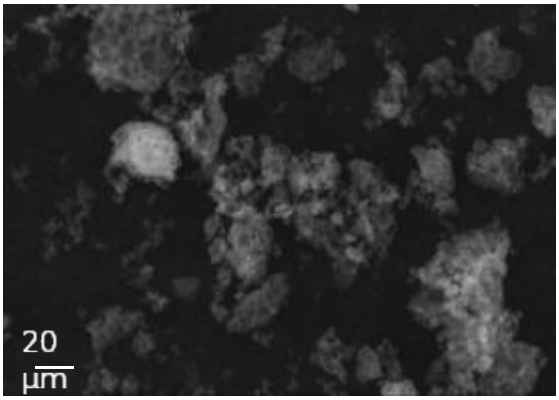

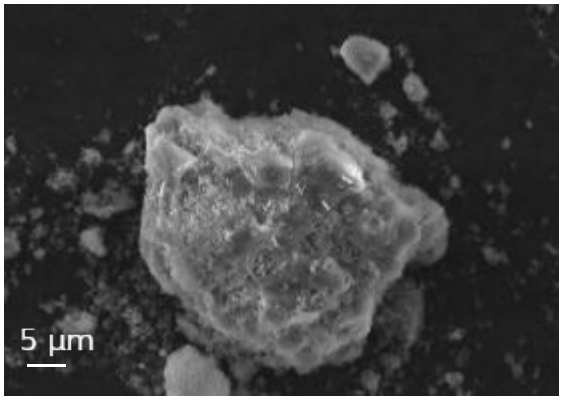

g h

Fig. 2. SEM images of Al_2O_3–Ag samples synthesized from precursors with various organic components: a, b – PVA, 850 °C; c, d – PVP, 850 °C; e, f – glycine, 850 °C; g, h – glycerol, 850 °C.

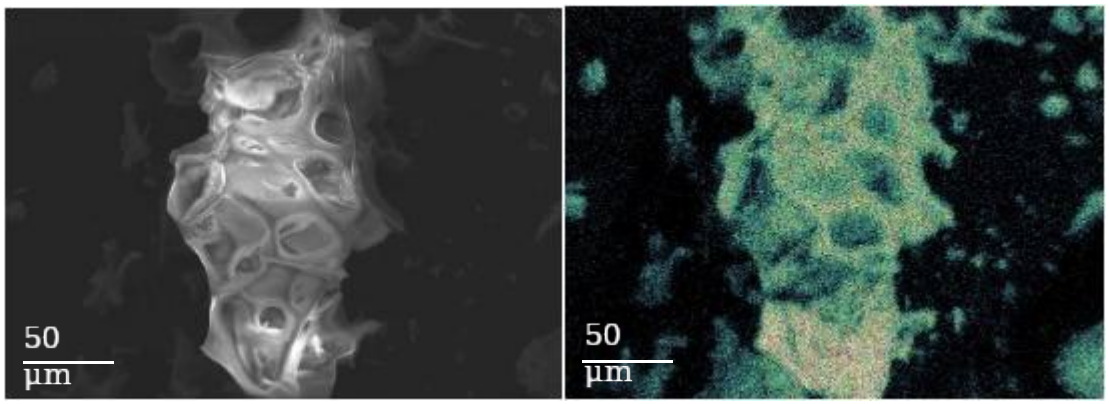

a b

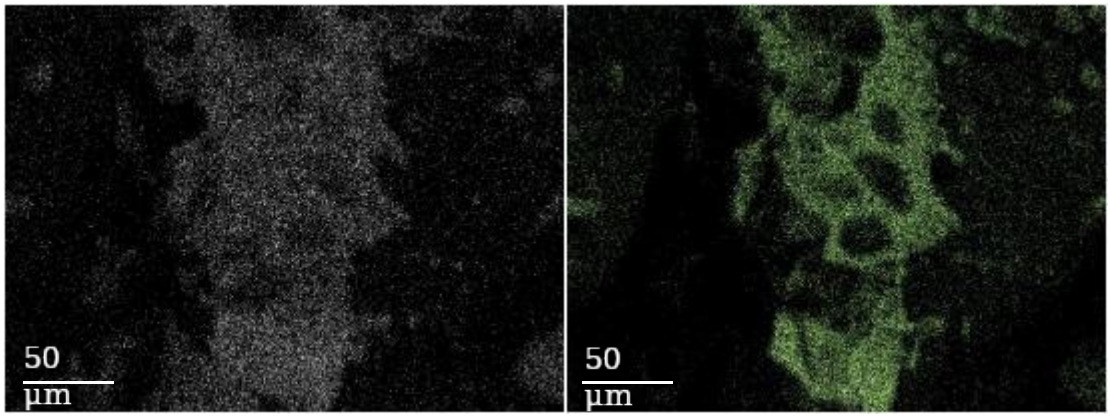

c d

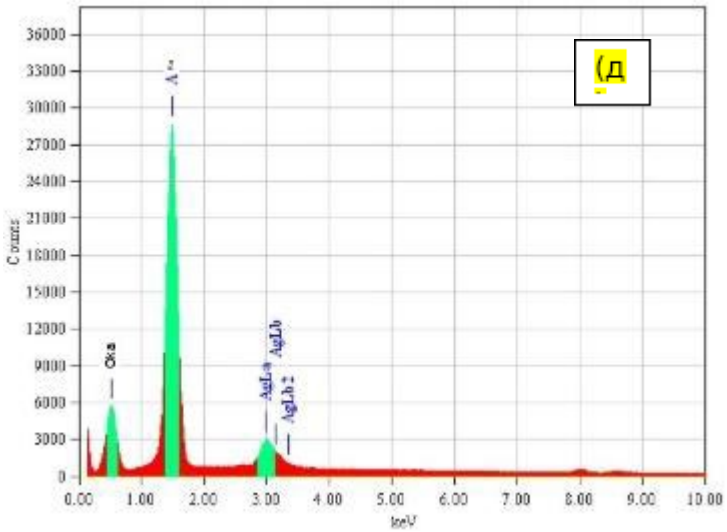

Fig. 3. Results of energy-dispersive analysis of Al_2O_3–Ag sample, PVP, 650 °C: a – SEM image; chemical element distribution maps b – Al, c – Ag, d – O; e – energy-dispersive spectrum.

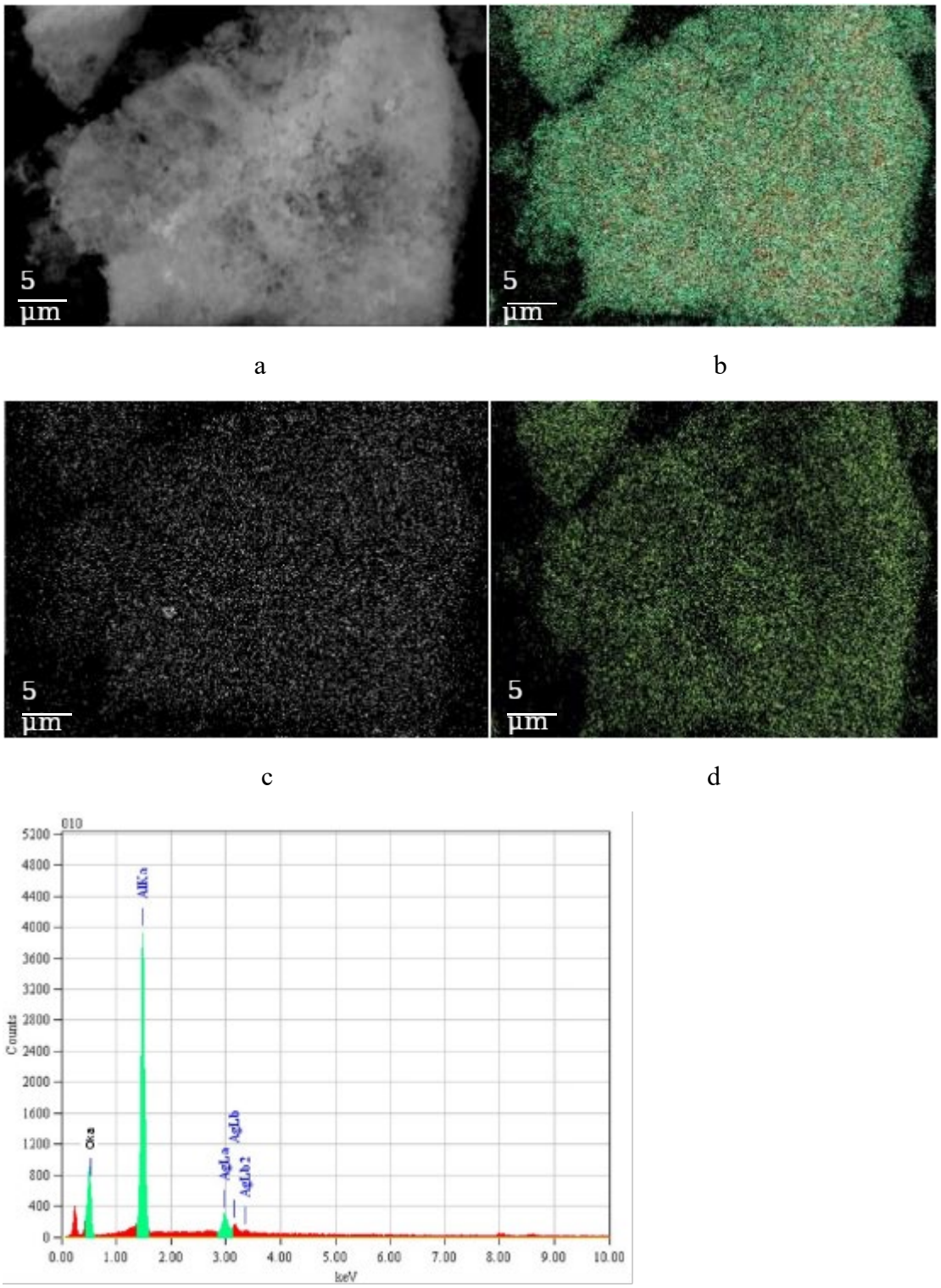

Fig. 4. Results of energy-dispersive analysis of Al_2O_3–Ag sample, glycerol, 850 °C: a – SEM image; chemical element distribution maps b – Al, c – Ag, d – O; e – energy-dispersive spectrum.

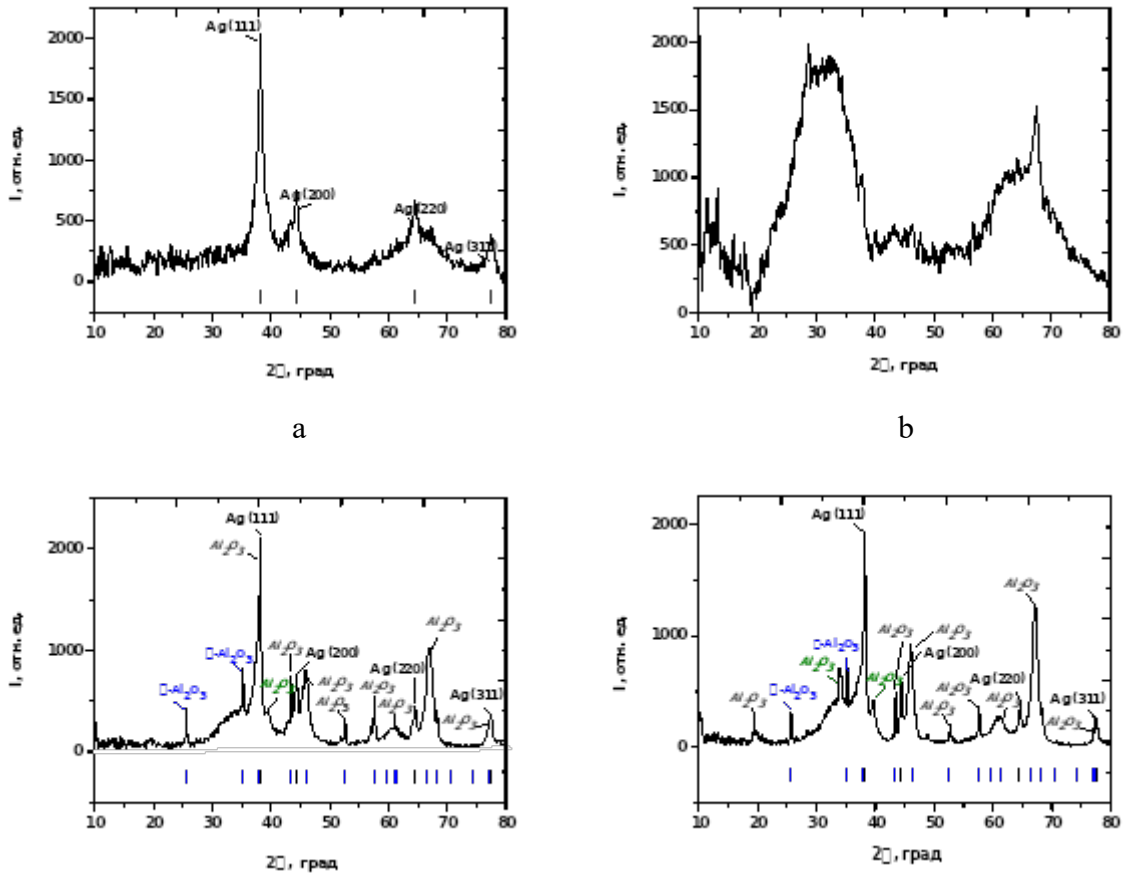

Fig. 5. X-ray diffraction patterns of Al_2O_3–Ag samples synthesized from precursors with various organic components: a – PVA, 650 °C; b – PVP, 650 °C; c – PVA, 850 °C; d – PVP, 850 °C (dash diagrams indicate phases of metallic silver (COD ID: 1100136) (black), α-Al_2O_3 (COD ID: 1000017) (blue)).

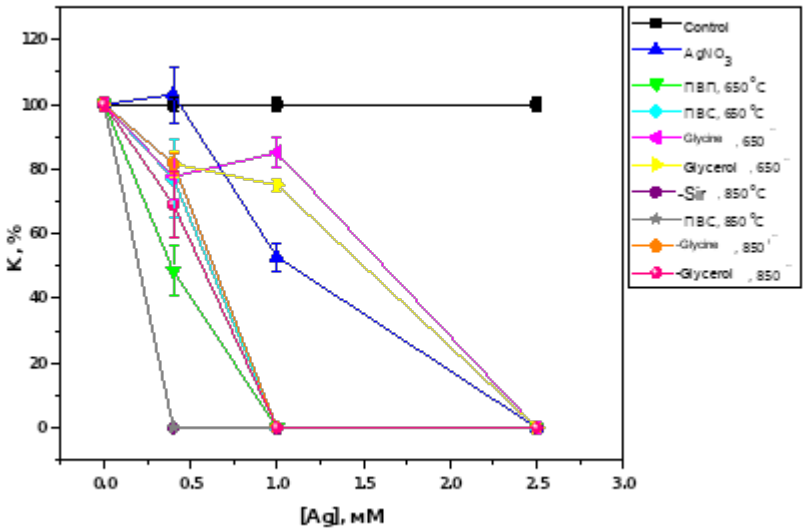

Fig. 6. Concentration dependences of the percentage ratio of colony-forming units in the studied samples synthesized with various organic components to the number of colony-forming units in the control experiment.